



ARID Journals

ARID International Journal for Science and Technology (AIJST)

ISSN: 2662-009X

Journal home page: <http://arid.my/j/aijst>

ARID

International Journal for Science and Technology
مجلة أريد الدولية للعلوم والتكنولوجياVOL.6 NO.12 DECEMBER 2023
ISSN: 2662-009XARID
ARID PUBLICATIONS
ARID MYCNET

مجلة أريد الدولية للعلوم والتكنولوجيا

المجلد 6 ، العدد 12 ، كانون الأول 2023 م

Study the Effect of Texture Extending Direction in Inpainting Missing Areas of Digital Images Using Modified Isotropic Model

Zainab A. Abdul Karim^{1,*}, Ahmed K Al-Jaberi².

1. Department of Mathematics, College of Science, University of Basrah, Basra, Iraq.
2. Department of Mathematics, College of Education for Pure Science, University of Basrah, Basra, Iraq.

دراسة تأثير اتجاه امتداد النسيج في طلاء الداخلي للمناطق المفقودة في الصور الرقمية باستخدام نموذج isotropic المعدل

- زينب علي عبدالكريم^{1,*}, احمد كاظم الجابري²
1. قسم الرياضيات , كلية العلوم , جامعة البصرة , البصرة , العراق.
 2. قسم الرياضيات , كلية التربية للعلوم الصرفة , جامعة البصرة , البصرة , العراق.

zaynab.eali.sci@uobasrah.edu.iq

arid.my/0008-7365

<https://doi.org/10.36772/arid.aijst.2023.6126>

ARTICLE INFO

Article history:

Received 01-11-2023

Received in revised form 14-11-2023

Accepted 22-11-2023

Available online 15-12-2023

<https://doi.org/10.36772/arid.ajst.2023.6126>

ABSTRACT

The modified isotropic model was used to recover the missing regions of the colored stripes image, and two models (the isotropic model and the modified isotropic model) were applied to them. Comparing the results obtained from the two models show that the modified model achieved better results than the results of the old model. A study was also conducted on the effect of the texture direction in the missing area on the success of the modified model. Use a number of image quality measures, including MSE, PSNR, and SSIM.

المخلص

تم استخدام نموذج الخواص المعدل لاستعادة المناطق المفقودة من صورة الخطوط الملونة، وتم تطبيق نموذجين عليها (النموذج الخواص والنموذج الخواص المعدل). وبمقارنة النتائج التي تم الحصول عليها من النموذجين أظهرت أن النموذج المعدل حقق نتائج أفضل من نتائج النموذج القديم. كما أجريت دراسة تأثير اتجاه النسيج في المنطقة المفقودة على نجاح النموذج المعدل. استخدم عددًا من مقاييس جودة الصورة، بما في ذلك **MSE** و **PSNR** و **SSIM**.

1. Introduction

The image is a means of expression and communication that replaces many other means of communication. However, sometimes some information is lost from the image due to a variety of reasons, such as poor storage and weather conditions. Image inpainting is a method that aims to repair the damaged part of an image in order to rebuild it and provide a high-quality semantic approximation of the original image [1].

First, Masnou and Morel (1998) modified the diffusion-based approach in which the level lines-based disocclusion produces a result with severe discontinuities [2]. In 2000, Bertalmio et al. addressed the inpainting process using diffusion Partial Differential Equation (PDE), in which boundary information propagates along the direction of isophotes into the region to be inpainted [3].

Additionally, Bertalmio presented an iterative algorithm based on PDEs. This method was inspired by the techniques of museum artisans [3] who diffused pixels automatically using the isophotes process, which enables the simultaneous filling of missing areas in any direction without limitation on the area to be inpainted.

To achieve this, a smoothness estimator may be introduced during computation, and the diffused information is along the isophote. Moreover, a time-varying estimator along the isophote direction determines the spatial change based on a discretization gradient vector. Due to anisotropic diffusion, the technique is effective on images with small fractures but produces a blurring effect when larger mask regions are used.

In addition, it cannot be used to restore large textured areas or images with several damaged parts. The Total Variation (TV) model was suggested by Chan and Shen (2001) [4] for inpainting.

Based on the application strength of isophotes, this area is usually the Euler-Lagrange equation and anisotropic diffusion. In addition, Oliveira et al(2001) [5] offer a convolution-based algorithm for rapid image inpainting. In their approach, the to-be-inpainted areas are periodically convolved with a predefined diffusion mask.

This model matches isotropic diffusion closely. This method considers the center weight of the diffusion mask to be zero since the original image pixel to which it corresponds is unknown. The TV model was extended to the CDD (Curvature Driven Diffusion) model in 2001 [6] which included the isophote curvature information to handle curved structures more effectively. Then, Telea (2004) [7] developed a fast marching approach in which, in this category, image contents diffuse smoothly from boundary areas towards the interior of the missing area, however this model is more time-consuming than previously published models and has certain problems when applied to a wide area.

In the year of 2007, Charles K. Chui and J. Wang investigated the total energy function in the wavelet domain [8]. Hadhoud et al. (2008) proposed a change to the Oliveira method that reduces implementation time [9]. The convolution-based algorithms are rapid, but they do not perform well in images with damaged edges and strong contrast. Based on the change of the convolution step, this approach modifies the Oliveira algorithm to minimize inpainting time and improve the quality of the results. Based on a mixture of wavelet decomposition, a novel approach for digital inpainting. C.H. Hagiwara et al. (2009) [10].

propose surface-based inpainting and texture synthesis. The authors of [11] suggested a convolution-based inpainting approach that employed an adaptive kernel to improve processing of edge areas by using the gradient of known pixels in the area of the missing pixel to compute weights in the convolving mask.

Due to the significant gradient values in the edge areas, the contribution of pixels adjacent to the edges must be less than that of pixels in smooth areas. According to zero or small weights of missing pixels' neighbors with significant local gradients, edges will be better retained.

Consequently, the method can estimate the missing pixels while keeping the image's sharp edges. While performing convolution on images with damage using two mask functions.

In 2011, H. Noori et al. [12] presented bilateral filtering, a convolution-based approach using an edge-preserving smoothing filter. By applying two Gaussian filters to a localized pixel neighborhood, one in the intensity domain and the other in the spatial domain that retains sharp edges, the bilateral filter replaces a pixel's value with the average weight of its neighbors in both space and range. The mask functions are useful for repairing the damaged regions.

Chan, Raymond H, and others suggest in [13] an Alternating Direction Method for Image Inpainting (2011). Using wavelet and image decomposition, texture inpainting, and structure inpainting, the authors of [14] proposed a method for recovering images. Using the wavelet transform, the original image was split into four pieces in order to preserve image information and reconstitute high-quality data. Li et al. (2017) [15] used PDE in combination with smooth constraints as a method of regularization to diffuse the local information. Thus, the algorithm will follow to the instructions provided by the local structure and iteratively regularize, resulting in a series of continuous, smooth images.

Consequently, information appearing on a local pixel on an image contour diffuses the smoothness along the direction of the contour and not across borders, addressing the shortcomings of the most recent approaches by Bertalmio et al. [3].

In both directions, pixels located on uniform surfaces will degrade smoothness. Thus, the combination of isophotes and PDEs produces an inpaint image with a constant evolution structure. However, these strategies are costly compared of the tardy introduction of buildings in border regions. Sridevi and Kumar proposed using fractional-order derivatives with discrete Fourier transform (DFT) for the inpainting work in 2019 [16].

The method employs a fractional-order nonlinear diffusion model that is difference curvature driven by Chen et al. [10] to manage gap areas and a fractional-order variational model to eliminate image noise and blurring. This approach can retain edges during the image restoration process.

However, this approach relies on human intervention for the manual selection of fractional orders, which might result in a subpar performance in inpainted regions.

The current study included a study of the effect of texture orientation on the efficiency of the proposed model in restoring deleted areas using vertical and horizontal textures were tested.

2. Image Quality Assessment

Three different statistical quality measurements are used to assess the quality of inpainted images.

1. Mean Square Error (MSE) is one of the important quality measurements and it can be applied to find the difference between the inpainted image I' and the original one I . The MSE is given by [17][18]:

$$MSE = \frac{1}{(NMR)} \sum_{q=1}^R \sum_{n=1}^N \sum_{m=1}^M [I_q(n, m) - I'_q(n, m)]^2 \quad 1$$

Where R is the number of channels in a color image, N is the number of rows and M is the number of columns in the channel.

2. The Peak Signal Noise Ratio (PSNR) is another quality measurement parameter that can be found in [17]:

$$PSNR = 10 \log_{10} \left(\frac{255^2}{MSE} \right) \quad 2$$

Better quality of the inpainted image is obtained when the value of PSNR is high and MSE is low.

3. The third parameter is Structural Similarity Index measure (SSIM)[18] which is used to measure the similarity between original and inpainted images.

The SSIM can be calculated by the relationship:

$$SSIM(I, I') = \frac{(2\mu_I\mu_{I'} + c_1)(2\sigma_{II'} + c_2)}{(\mu_I^2 + \mu_{I'}^2 + c_1)(\sigma_I^2 + \sigma_{I'}^2 + c_2)} \quad 3$$

where (μ_I, σ_I) and $(\mu_{I'}, \sigma_{I'})$ denote the mean and standard deviation of patches in the images I and I' , respectively; $\sigma_{II'}$: the covariance of I and I' ; $c_1 = (k_1h)^2$, $c_2 = (k_2h)^2$ such that $h = 2^{\text{bits per pixel}} - 1$, $k_1 = 0.01$ and $k_2 = 0.03$.

However, the value of SSIM is range from 1 to 0 where when the value is 1 means the two images are identical while 0 values refer to not identical. Therefore, the quality of inpainted images increases when the value of SSIM increases.

3. Isotropic model

Diffusion-based inpainting is the first model used to recover the damaged or missing part of the image by spreading information from the surrounding areas of the missing region at the pixel point [19]. However, isotropic diffusion is the second-order linear parabolic equation. Let $f \in L^2(\Omega)$ is an image and $D \subset \Omega$ is a missing information region from the original image; u is the inpainted image is given by the solution of the below equation[20] :

$$\begin{cases} u_t = \Delta u, & t \geq 0 \\ u(0, x, y) = 0. \end{cases} \quad 4$$

In addition, u can be calculated from the solution of minimization functional for the squared total variation. The formula of the heat equation can be introduced as minimization energy functional as [21]:

$$\min_{u \in L^2(\Omega)} \{ \iint |\nabla u|^2 \, dx dy, \text{ such that } u = f \text{ in } \Omega \setminus D \} \quad 5$$

Euler- Lagrange equation and gradient descent method are applied to the minimization functional 2, and we get

$$u_t = \Delta u \quad 6$$

The solution of equation 4 or 6 with the Dirichlet boundary condition is used to recover the missing regions in the image. The explicit finite difference method (EFDM) is applied to find the solution of equation 4 or 6, which is imitative of the solution of the heat equation on the spatial (image) domain. This equation has studied the spreading of temperatures (information) within a period in all directions based on the boundary condition[22]. However, the spread in all directions will cause failure to recover edge construction of the missing area and appear blurred under the isotropic model. The diffusion term comes from the idea of propagating local information with smoothness constraints by analogy with some physical phenomena like heat propagation in physical structures[2]. Isotropic diffusion acts as low-pass linear filtering suppressing high frequencies in the image thus, it works to minimize these variations in all directions that in turn led to appearing blurred close to edges and contours. More general formalisms using nonlinear PDEs are used for describing the physical and fluid dynamics phenomena to get better restoration of edges and more sharpness [9].

4. Modify the Isotropic Model

The isotropic diffusion model is modified by adding more than one algebraic expression to reduce the blur of the large missing area and enhance the edge of restoration. Modified isotropic model is modified by adding the first derivative of the missing area of the image [23]. The ability of the first derivative helps to build the edges and extend the isophote line, which improves recovering missing areas. The modified isotropic equation writes as follows:

$$u_t = \Delta u + \alpha u_x + \beta u_y, \quad t \geq 0 \quad 7$$

Where u_x and u_y are the first derivatives of the image, the α and β are coefficients. Furthermore, the value of α and β play an important effect in the values of quality measures.

5. Experiments and Results

The experiments that were conducted included selecting 10 different color stripes image selected from [24], Four types of masks of different sizes and shapes were used are case1(square)(see Fig.2b), case2(narrow rectangular)(see Fig.3b), case3 (vertical narrow rectangular)(see Fig.4 b), and case 4(large rectangular) (see Fig.5 b) shapes in the different sizes and locations of the image. And four types of masks. used the two models, the isotropic model and the modified model of the isotropic diffusion model, which was used to recover missing areas from images of colored striped.



Figure(1): Example of color stripes images

The Matlab programming was used to test the modified model on the selected standard striped color images. Two cases of α and β values are selected to test the modified model depending on the texture direction. When the texture direction is horizontally extended, the values of $\alpha=0$ and $\beta=1$ while $\alpha=1$ and $\beta=0$ are selected for the vertically extended texture direction.

6. Experimental Results of Color Striped Images

Color strip images (10 different images) are used to prove the behavior of the modified model and investigate its ability to enhance the inpainted images[24]. The experiments of color-striped images were conducted under the same dimensions and locations of the natural images. The images that were inpainted by using the isotropic model appeared blurry, for all areas of the missing region, while the recovery images by the modified model show better inpainted and visibility of the edges, especially in small and narrow missing areas. The best results were in the narrow and small areas the blurring increases when the missing area gets larger.

Figure 2a shows an original image containing vertical color strips and Fig.2b shows a square mask region. The missing region is inpainted using the isotropic model and the obtained image appeared blurred and unclear to edges as shown in Fig. 2c. However, using the modified isotropic model with $\alpha=1$ and $\beta=0$ appeared better restoration of the missing region with clearer edges as shown in Fig.2d. In case 2, the selected missing region is chosen as a narrow horizontal rectangular line as shown in Fig. 3b.

The restoration of the missing region and edges using the modified isotropic model with $\alpha=1$ and $\beta=0$ enhances the treated image where the edges appeared clearer with less blurry compared by the inpainted image using the isotropic model as shown in Fig. 3d.

Case 3 represented using a narrow vertical rectangular missing area and the inpainted area that construct using the original model appeared blurry with failure to restore the edges as seen in Fig. 4c. However, using the modified isotropic model with $\alpha=1$ and $\beta=0$ significantly reduced blurring and enhanced the recovery of the missing area as well as edges as shown in Fig. 4d.

Case 4 represents a large rectangular missing area extending horizontally on the image (Fig. 5b). The results of filling region using the isotropic model also appeared blurry with unclear edges and details of the inpainted area. However, when using the modified isotropic model $\alpha=1$ and $\beta=0$, the blurring significantly decreased and the edges appeared partially in the inpainted area as shown in Fig. 5c.

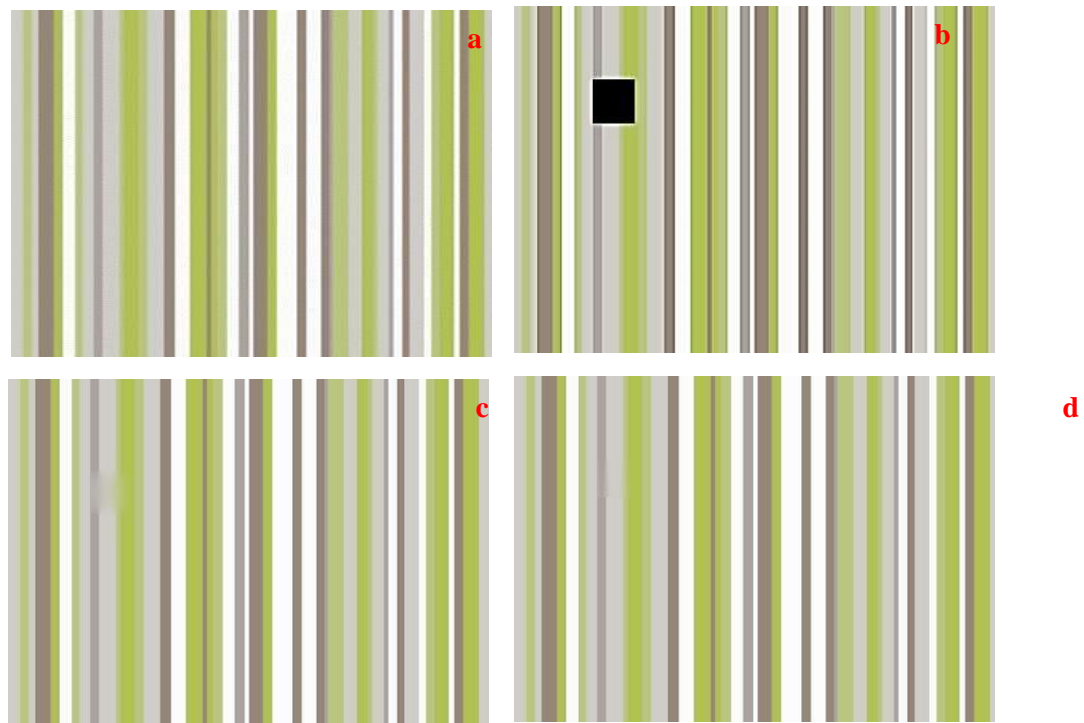
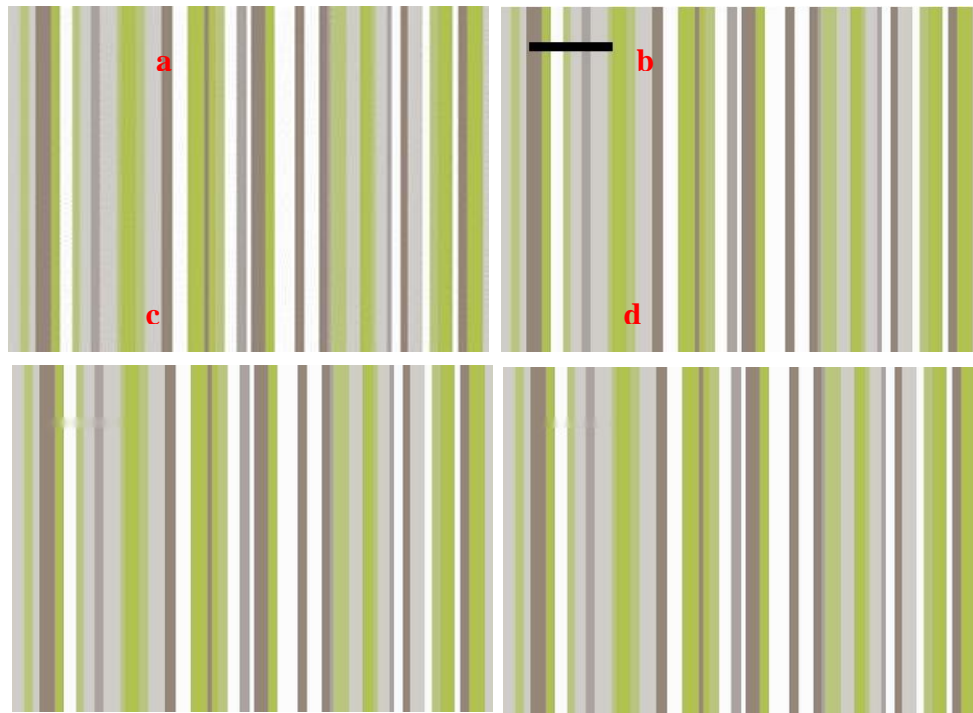


Figure2: Example of Case1 color stripes image, (a) original image, (b) square mask image, (c) image inpainted by isotropic model, (d) image inpainted by modified isotropic model $\alpha=1$ and $\beta=0$.



Figure(3): Example of Case2 color stripes image, (a) original image, (b) square mask image, (c) image inpainted by isotropic model and (d) image inpainted by modified isotropic model $\alpha=1$ and $\beta=0$.

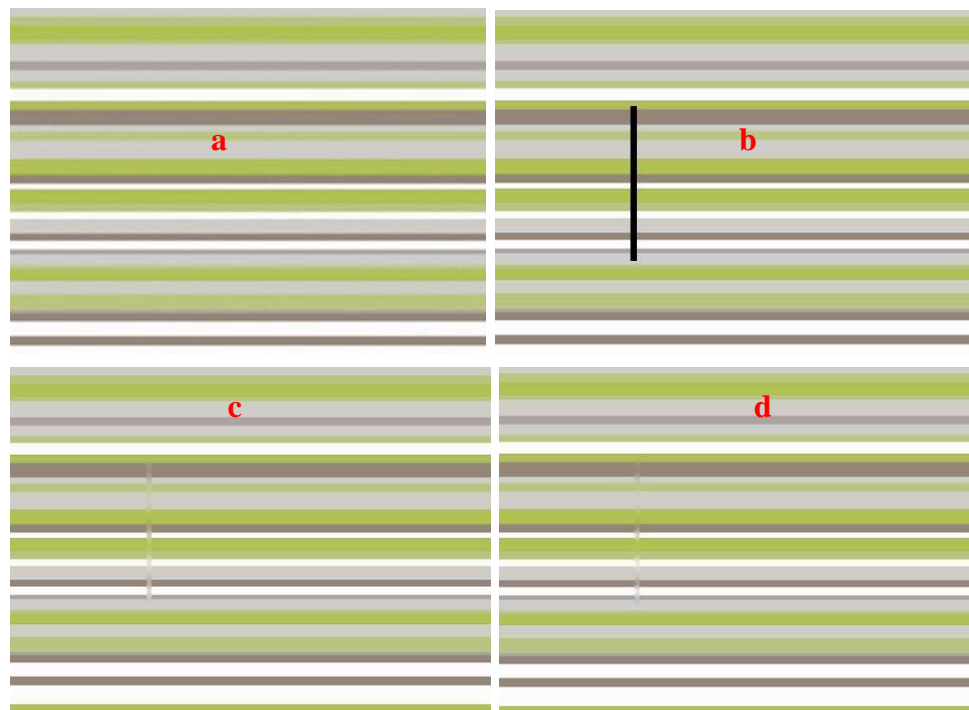


Figure 4: Case3 color stripes image, (a) original image, (b) square mask image, (c) image inpainted by isotropic model and (d) image inpainted by modified isotropic model $\alpha=0$ and $\beta=1$.



Figure5: Case4 color stripes image, (a) original image, (b) square mask image, (c) image inpainted by isotropic model and (d) image inpainted by modified isotropic model $\alpha=1$ and $\beta=0$.

Table 1 is listed the average values of the quality measures obtained for inpainted images using the modified isotropic model compared to the original isotropic model. From the results, can be noted that all quality measures are enhanced for the images that are inpainted using a modified model compared with the original model.

The MSE value decreased for all cases but for case1 and case 2 the reduced value was in a percentage of around 62% and 42.8%, respectively. Furthermore, the time of inpainted images by the modified isotropic model is highly reduced compared to the original isotropic model. For example, the time for treatment images using the modified model for case 1 was 1.3 sec compared to 40.6 sec for the same case when the original model is used to inpaint images.

Table(I): Image inpainted quality assessment comparison using averages of MSE, PSNR, and SSIM for color striped images

Cases	Isotropic Model				Modified Isotropic Model			
	MSE	PSNR	SSIM	Time (s)	MSE	PSNR	SSIM	Time (s)
Case1	56.601	31.211	0.729	40.6	21.580	35.710	0.895	1.316
Case2	44.146	32.145	0.798	3.013	25.245	34.591	0.887	0.897
Case3	45.574	31.650	0.736	7.312	37.300	32.501	0.808	2.930
Case4	92.212	28.807	0.497	356.7	81.593	29.210	0.546	9.872

In addition, this study was conducted on color-striped images to find out the effect of the texture direction on the results of applying the modified model. Two directions,(vertical and horizontal) and two different values of α and β as 0,1. Furthermore, the quality assessment values are also studied by changing the direction of texture using different values of α and β as 0,1.

Table 2 summarizes the measured MSE, when the change direction of texture decreases when the texture is vertical, $\alpha =1$ and $\beta =0$, while the amount of the mean square error increases when $\alpha =0$ and $\beta =1$ in all cases.

When the texture is horizontal direction and $\alpha =1$ and $\beta =0$ increases MSE values and decreases when $\alpha =0$ and $\beta =1$

Table (II): values of MSE when applying modified isotropic model with a different direction for the Experiment of color striped images

Cases	Vertical texture		Horizontal texture	
	$\alpha = 1, \beta = 0$	$\alpha = 0, \beta = 1$	$\alpha = 1, \beta = 0$	$\alpha = 0, \beta = 1$
Case1	21.580	104.602	104.602	21.580
Case2	22.576	79.155	94.768	7.654
Case3	13.183	123.896	83.639	38.343
Case4	83.516	112.042	123.814	46.800

Table 3 summarizes the measured PSNR, when the change direction of texture increases when the texture is vertical, $\alpha = 1$ and $\beta = 0$, while the amount of PSNR decreases when $\alpha = 0$ and $\beta = 1$ in all cases. When the texture is a horizontal direction and $\alpha = 1$ and $\beta = 0$ decreases PSNR values and increase when $\alpha = 0$ and $\beta = 1$

Table (III): values of PSNR when applied modify isotropic model with different direction for Experiment of color striped images:

Cases	Vertical Texture		Horizontal Texture	
	$\alpha = 1, \beta = 0$	$\alpha = 0, \beta = 1$	$\alpha = 1, \beta = 0$	$\alpha = 0, \beta = 1$
Case1	35.710	30.544	30.544	35.710
Case2	35.166	29.519	31.252	42.444
Case3	40.246	29.575	29.113	32.651
Case4	29.113	27.988	29.757	32.043

Table 4 summarizes the measured SSIM, when the change direction of texture increases when the texture is vertical, $\alpha = 1$ and $\beta = 0$, while SSIM decreases when $\alpha = 0$ and $\beta = 1$ in all cases. when the texture is a horizontal direction and $\alpha = 1$ and $\beta = 0$ decreases SSIM values and increase when $\alpha = 0$ and $\beta = 1$

Table (IV): values of SSIM when applying modified isotropic model with a different direction for the Experiment of color striped images:

cases	Vertical Texture		Horizontal Texture	
	$\alpha = 1, \beta = 0$	$\alpha = 0, \beta = 1$	$\alpha = 1, \beta = 0$	$\alpha = 0, \beta = 1$
Case1	0.895	0.458	0.458	0.895
Case2	0.896	0.495	0.314	0.984
Case3	0.978	0.178	0.450	0.785
Case4	0.549	0.408	0.456	0.769

Table 5 shows values of time, when the change direction of texture increases when the texture is vertical, $\alpha = 1$ and $\beta = 0$, while decreases when $\alpha = 0$ and $\beta = 1$ in all cases. when the texture is a horizontal direction and $\alpha = 1$ and $\beta = 0$ decreases time values and increase when $\alpha = 0$ and $\beta = 1$

Table (V): values of Time when applying modified isotropic model with a different direction for the Experiment of color-striped images:

Cases	Vertical Texture		Horizontal Texture	
	$\alpha =1, \beta =0$	$\alpha =0, \beta =1$	$\alpha =1, \beta =0$	$\alpha =0, \beta =1$
Case1	2.246	2.408	2.409	1.432
Case2	1.267	1.348	6.928	1.234
Case3	4.016	15.216	4.970	2.200
Case4	16.292	19.208	16.559	8.459

7. Conclusions

The modified isotropic model is used for restoring the missing region of the digital image where this model is tested to restore four shapes of masks (missing area). The results obtained by the modified isotropic model are compared with the obtained results using the isotropic model. To begin with, the isotropic model appeared more effective in reconstructing the small and narrow missing areas than large and wide areas but the model failed to restore the edges. Secondly, the modified isotropic model was applied to 10 striped color images with the same masks used in the isotropic model. The modified model was effective in revealing details and edges and reducing blurring for inpainted missing areas.

The modified isotropic model was introduced by adding the first derivative in the directions of the x and y, which discovered a relationship between the coefficients of the added parts and the direction of the texture in the image to be restored, which helped to improve the restoring missing regions in the texture images. Furthermore, there was an improvement in the results by visual inspection of images and quality statistical measures where a decrease in MSE and an

increase in both PSNR and SSIM for all types of inpainted image. In future, different database will be tested to check the efficiency and effective of the modified isotropic model.

Abbreviation Table:

Abbreviation	DESCRIPTION
MSE	Mean Square Error
PSNR	The Peak Signal Noise Ratio
SSIM	Structural Similarity Index measure
PDE	Partial Differential Equation
TV	Total Variation
CDD	Curvature Driven Diffusion
EFDM	The explicit finite difference method

References

- [1] Z. Qin, Q. Zeng, Y. Zong, and F. Xu, "Image inpainting based on deep learning: A review," *Displays* 102028 (2021) 69
- [2] S. Masnou and J.-M. Morel, "Level lines based disocclusion," in *Proceedings 1998 International Conference on Image Processing. ICIP98 (Cat. No. 98CB36269)* 259–263 (1998),
- [3] M. Bertalmio, G. Sapiro, V. Caselles, and C. Ballester, "Image inpainting," in *Proceedings of the 27th annual conference on Computer graphics and interactive techniques* (2000), 417–424
- [4] T. Chan, "Local inpainting models and TV inpainting," *SIAM J. Appl. Math.*, 62, no. 3, (2001) 1019–1043
- [5] M. Richard and M. Y.-S. Chang, "Fast digital image inpainting," in *Appeared in the Proceedings of the International Conference on Visualization, Imaging and Image Processing (VIIP 2001), Marbella, Spain (2001)* , 106–107
- [6] T. F. Chan and J. Shen, "Nontexture inpainting by curvature-driven diffusions," *J. Vis. Commun. Image Represent*, 12, no. 4,. (2001) 436–449
- [7] A. Telea, "An image inpainting technique based on the fast marching method," *J. Graph. Tools* 9, no. 1, (2004) 23–34
- [8] C. K. Chui and J. Wang, "Wavelet-based minimal-energy approach to image restoration," *Appl. Comput. Harmon. Anal.*, 23, no. 1, (2007) 114–130
- [9] M. M. Hadhoud, K. A. Moustafa, and S. Z. Shenoda, "Digital images inpainting using modified convolution based method," *Int. J. signal Process. image Process. pattern Recognit*, 1, no. 1,. (2008) 1–10
- [10] H. Chen, I. Hagiwara, and A. K. Tieu, "Image reconstruction based on combination of wavelet decomposition, inpainting and texture synthesis," *Int. J. Image Graph*, 9, no. 01,. (2009) 51–65
- [11] H. Noori, S. Saryazdi, and H. Nezamabadi-Pour, "A convolution based image inpainting," in *1st International Conference on Communication and Engineering*, vol. 1, no. 2 (2010),
- [12] H. Noori, S. Saryazdi, and P. H. NEZAMABADI, "A bilateral image inpainting," *IJST, Transactions of Electrical Engineering* 35, no. E, (2011), 295-108
- [13] R. H. Chan, J. Yang, and X. Yuan, "Alternating direction method for image inpainting in wavelet domains," *SIAM J. Imaging Sci*, 4, no. 3,. (2011) 807–826
- [14] H. Zhang and S. Dai, "Image inpainting based on wavelet decomposition," *Procedia Eng.* 29, (2012) 3674–3678
- [15] H. Li, W. Luo, and J. Huang, "Localization of diffusion-based inpainting in digital images," *IEEE Trans. Inf. forensics Secur.*, 12, no. 12,. (2017) 3050–3064
- [16] G. Sridevi and S. Srinivas Kumar, "Image inpainting based on fractional-order nonlinear diffusion for image reconstruction," *Circuits, Syst. Signal Process.*, 38, no. 8, (2019) 3802–3817
- [17] A. Halim and B. V. R. Kumar, "An anisotropic PDE model for image inpainting," *Comput. Math. with Appl.*, 79, no. 9,. (2020) 2701–2721
- [18] Z. Wang, A. C. Bovik, H. R. Sheikh, and E. P. Simoncelli, "Image quality assessment: from error visibility to structural similarity," *IEEE Trans. image Process.* 13, no. 4, (2004) 600–612

- [19] K. R. Patel, L. Jain, and A. G. Patel, "Image inpainting-a review of the underlying different algorithms and comparative study of the inpainting techniques," *Int. J. Comput. Appl.* 118, no. 10, (2015) 32 – 38
- [20] C. Guillemot and O. Le Meur, "Image inpainting: Overview and recent advances," *IEEE Signal Process. Mag.* 31, no. 1, (2013)127–144
- [21] A. K. Al-Jaberi and E. M. Hameed, "A Review of PDE Based Local Inpainting Methods," in *Journal of Physics: Conference Series* 12149 (2021) 1818, no. 1,
- [22] G. Aubert, P. Kornprobst, and G. Aubert, "Mathematical problems in image processing: partial differential equations and the calculus of variations", Springer 95 (2006) 147,
- [23] Z. A. A. Kareem and A. K. Al-Jaberi, "A Novel Image Inpainting Technique Based on Isotropic Diffusion," *Basrah J. Sci.* 40, no. 2. (2022) 289–305 .
- [24] M. Cimpoi, S. Maji, I. Kokkinos, S. Mohamed, and A. Vedaldi, "Describing textures in the wild," in *Proceedings of the IEEE conference on computer vision and pattern recognition* (2014), 3606–3613